



Why the Mixed Layer Depth Matters When Diagnosing Marine Heatwave Drivers Using a Heat Budget Approach

Youstina Elzahaby^{1,2*}, Amandine Schaeffer^{1,2}, Moninya Roughan^{1,2} and Sébastien Delaux³

¹ Coastal and Regional Oceanography Lab, School of Mathematics and Statistics, University of New South Wales, Sydney, NSW, Australia, ² Centre for Marine Science and Innovation, University of New South Wales, Sydney, NSW, Australia,

³ Meteorological Service of New Zealand, Wellington, New Zealand

OPEN ACCESS

Edited by:

Thomas Wernberg,
University of Western Australia,
Australia

Reviewed by:

Susan Kay,
Plymouth Marine Laboratory,
United Kingdom
Tomomichi Ogata,
Japan Agency for Marine-Earth
Science and Technology (JAMSTEC),
Japan

*Correspondence:

Youstina Elzahaby
y.elzahaby@unsw.edu.au

Specialty section:

This article was submitted to
Climate, Ecology and People,
a section of the journal
Frontiers in Climate

Received: 17 December 2021

Accepted: 09 February 2022

Published: 25 March 2022

Citation:

Elzahaby Y, Schaeffer A, Roughan M
and Delaux S (2022) Why the Mixed
Layer Depth Matters When
Diagnosing Marine Heatwave Drivers
Using a Heat Budget Approach.
Front. Clim. 4:838017.
doi: 10.3389/fclim.2022.838017

Marine heatwaves (MHWs) are extreme warming events that can result in significant damage to marine ecosystems and local economies. The primary drivers of these events have been frequently studied using an upper ocean heat budget. However, various surface mixed layer (SML) depths have been used with little attention paid to the impact of the depth chosen on heat budget term estimates. We analyse MHW drivers in two dynamically contrasting regions off the east coast of Australia (East Australian Current extension) and the west coast of New Zealand over a 30-year period (1985–2014, inclusive). We compare the magnitude of the air-sea heatflux and advection terms in a volume-averaged heat budget using three different SML depth estimates. We show that the SML depth over which the heat budget is calculated has direct consequences on the identification of MHW dominant drivers. The air-sea heatflux term is amplified when the SML depth is underestimated and dampened when overestimated. The variation in the magnitude of the advection term is dependent on the barotropic or baroclinic structure of the currents. We, also, show that the impact on MHW driver classification is both temporally and regionally dependent. Generally, a deep SML estimate results in more MHWs being classified as advection and less classified as air-sea heatflux-driven. However, during the cool months, a shallow estimate produces the opposite pattern and to a varying degree of intensity depending on the region's dynamics. Use of daily and spatially variable SML depth in a heat budget calculation allows the comparison between regions with different dynamics influencing the mixed layer depth. These results show that when using a heat budget approach to explore marine heatwaves over extended time and space (e.g., regions and seasons), it is imperative to consider the temporal and spatial variability in the SML depth.

Keywords: air-sea heatflux, advection, mixed layer depth, East Australian Current, heat budget, dominant drivers, surface mixed layer, marine heatwaves

1. INTRODUCTION

Marine heatwaves (MHWs) are discrete, prolonged anomalously warm water events (Hobday et al., 2016, 2018) that can have devastating consequences on ocean ecosystems. Impacts that have been reported include marine organism mortality and ecosystem redistribution (Wernberg et al., 2013; Salinger et al., 2019; Smale et al., 2019) resulting in financial burdens on local fisheries and governments (Mills et al., 2013). These events are not necessarily restricted to the surface (Oliver et al., 2017), but rather can reach their maximum temperature intensity in the ocean sub-surface (Benthuyzen et al., 2018; Elzahaby and Schaeffer, 2019), in particular near the thermocline (Schaeffer and Roughan, 2017). Extremely warm temperature anomalies during MHWs are often restricted to the surface mixed layer (SML) being the turbulent surface layer within which temperature and salinity are well mixed and close to vertically uniform. However, extreme temperature anomalies have also been detected at ocean depths of hundreds of meters (Elzahaby et al., 2021). Moreover, sub-surface warming that penetrates the SML can persist at depth, linger past the disappearance of the surface signal and become re-entrained into the surface layers in a subsequent season (Deser et al., 2003; Jackson et al., 2018; Scannell et al., 2020).

During a MHW, the depth extent of the elevated temperature anomalies is linked to the event's primary driver (Elzahaby et al., 2021). Primary drivers of MHWs range from atmospheric (Chen et al., 2014; Benthuyzen et al., 2018) and local oceanic forcing (Oliver et al., 2017; Gawarkiewicz et al., 2019) to large-scale forcing *via* tele-connections (Feng et al., 2013). On a large scale, remote influences like El Niño-Southern Oscillation (ENSO) have been linked to sea surface temperature (SST) variation (Feng et al., 2013; Sen Gupta et al., 2020), whilst Rossby waves can modulate the mixed layer depth (MLD, Bowen et al., 2017; Li et al., 2020). Focusing on local processes, Elzahaby et al. (2021) showed that, on average in the Tasman Sea, anomalous warming from local advection-driven MHWs is four times deeper than atmospheric-driven events, which are mostly restricted to the surface layers. The impact of atmospheric forcing is almost entirely restricted to the SML (Chen et al., 1994) unlike oceanic advection, which is linked to the ocean dynamics. The impact of oceanic forcing can affect the ocean at any depth and especially when associated with deep mesoscale eddy structures (Rykova and Oke, 2015). That is, accounting for the depth extent of the ocean SML relative to the primary drivers of MHWs is imperative in understanding the respective impact of the forces that generate a MHW event.

Heat budgets have been used to describe the contribution of atmospheric and oceanic processes in the SML and the dominant drivers in the evolution of MHWs. Generally, heat budgets describe the processes that affect the temperature tendency including horizontal and vertical ocean advection, air-sea heatflux, entrainment of water into the mixed layer and horizontal and vertical mixing (diffusion). This diagnostic tool has often been used to identify the dominant drivers (Chen et al., 2015; Bowen et al., 2017) or the evolution of the different mechanisms influencing the temperature variation

during MHWs (Chen et al., 2015; Oliver et al., 2017). The mixed layer heat budget is usually volume-averaged over a fixed depth used as an estimate of the SML with the assumption that the temperature is homogeneous in the surface layers. The range of fixed depths used varies from approximately 50 m (Benthuyzen et al., 2014; Fathrio et al., 2018) to 250 m (Bowen et al., 2017). In some cases (e.g., Marin et al., 2021), heat budgets have been applied over large spatial and temporal scales (e.g., globally, from the coastal to deep ocean, over decades), without consideration of the variability in MLD between regions and seasons, but it is not clear what impact the constant SML has on the heat budget estimates.

The main temporal variability of the MLD is linked to the many processes occurring in the mixed layer (surface forcing, advection, internal waves, etc.) and ranges from diurnal (Brainerd and Gregg, 1995) to interannual variability including seasonal and intraseasonal variability (Kara, 2003). The vertical seasonal variability of the MLD, globally, is large and can range from less than 20 m in the summer to 500 m in the winter, whilst spring and autumn are transitional periods in between (Monterey and Levitus, 1997).

Biological activity is almost entirely restricted to the upper ocean which makes understanding the SML depth essential for understanding the ecosystem (Polovina et al., 1995). Moreover and for our purpose, information on the SML, including diagnostics of atmosphere and ocean variability within it, is essential in understanding the role of different mechanisms in the evolution of MHWs (e.g., Bond et al., 2015; Chen et al., 2015).

There is no single objective criterion for the SML depth, rather a variety of definitions are used with emphasis on differing criteria depending on the purpose of the analysis. Parameters used to define the SML include temperature, salinity and density criteria, calculated over various time scales (e.g., daily, monthly, seasonally) using gradient or threshold methods to define. Some typical examples include Kara et al. (2000), who used a temperature-based threshold approach and showed that a value of $\Delta T = 0.8^\circ\text{C}$ was an optimal estimate of turbulent mixing penetration (mixed layer activity) where ΔT is the temperature difference with respect to a fixed depth. Levitus (1982), using a density threshold, found a threshold value of $\Delta\sigma = 0.125 \text{ kg m}^{-3}$ which corresponds to the water-mass characteristics of Subtropical Mode Water in the North Atlantic, whilst Ohlmann et al. (1996) chose 0.5 kg m^{-3} based on extensive study of the penetration of shortwave radiation in the upper ocean. Gradient methods aim to identify the depth at which a strong variation occurs, assuming this is the base of the mixed layer. Values for the gradient method range from 0.0005 to 0.05 kg m^{-4} for density and $0.025^\circ\text{C m}^{-1}$ for temperature (Dong et al., 2008). Using threshold criteria, de Boyer Montégut et al. (2004) defined the SML depth as the value of temperature or density where $\Delta T = 0.2^\circ\text{C}$ or $\Delta\sigma = 0.03 \text{ kg m}^{-3}$, respectively. The authors used a reference depth at 10m, so as to avoid a large part of the strong diurnal cycle in the top few metres of the ocean, and identified the MLD as the depth at which one of the thresholds was exceeded. Most of these methods capture the regional characteristics and the temporal variability of the SML depth.

Here, we show analysis that illustrates the sensitivity of MHW driver classification to the choice of SML depth used in a heat budget. We investigated 82 MHW events in two dynamically different regions of the Tasman Sea (Figure 1). We compare heat budget results in three scenarios: a near-realistic scenario using a daily varying SML depth (MLD_V) based on de Boyer Montégut et al. (2004) as a benchmark for comparison with two constant scenarios of fixed depths at 30 m (MLD_{30}) and 150 m (MLD_{150}). We, further, compare the discrepancy in MHW dominant driver detection across the three scenarios. We present the results in the form of two focus case studies, one for each of the regions of interest, then we show the results on a statistical scale over a 30-year period (1985–2014) from the output of an eddy resolving ocean model. Finally, we discuss the results in the context of the impact of classifying MHW drivers across regions and seasons.

2. MATERIALS AND METHODS

2.1. Region and Model Data

For this analysis, we used model output from the Bluelink Ocean Forecasting Australia Model (OFAM3) which is an eddy-resolving (0.1° resolution) near global model. The model covers the period of 1985–2014 with daily resolution and 5 m vertical resolution in the upper layers increasing with depth (Oke et al., 2013). We used data output from a free-running model because some assimilation approaches can violate conservation principles and as such, introduce uncertainty in the heat budget (Stammer et al., 2016). Elzahaby et al. (2021) have previously used this model for heat budget analysis of MHWs after validation with Argo and satellite data.

We chose two sub-regions in the Tasman Sea that represent contrasting dynamical regimes (Figure 1). These are an “Eddy box” located in the eddy field south of the East Australian Current (EAC) separation (bounded by $151.2^\circ - 153.2^\circ E$ and $35^\circ - 37^\circ S$) and a “New Zealand box” located off the west coast of the North Island of New Zealand (bounded by $170^\circ - 172^\circ E$ and $38^\circ - 34^\circ S$), hereafter, referred to as Eddy and NZ boxes, respectively.

In the western Tasman Sea, the East Australian Current (EAC) is a highly energetic western boundary current that is characterized by strong SST variability (Ridgway and Dunn, 2003, Figures 1C,D). The Eddy box is in a region that is characterized by the presence of a large number of anticyclonic eddies shed from the EAC (Tranter et al., 1980), which result in frequent, deeper surface mixing (Tilburg et al., 2002), and captures the extreme temperature anomalies in the eddy field of the EAC southern extension. Here, the MLD ranges between 30 m in summer and 150 m in winter (Figure 1) due to high seasonal variability and pole-ward penetration of the EAC eddies in the southeastern Australia region (Condie and Dunn, 2006). Consequently, it has been shown that MHWs in the Eddy box are mostly driven by ocean advection (Elzahaby et al., 2021).

In the eastern Tasman Sea off the west coast of New Zealand, the temperature is comparatively more stable than the western Tasman Sea (Heath, 1981). The MLD varies between 20 m in summer and 100–150 m in winter (Figure 1) in close agreement with findings from Rahmstorf (1992). It has been shown that

MHWs in the NZ box are mostly driven by air-sea heat flux anomalies (Elzahaby et al., 2021).

2.2. Marine Heatwave Definition

MHWs were defined, as per (Hobday et al., 2016), as periods when the mean temperature in the SML (using a daily varying MLD) exceeded the 90th percentile for a consecutive 5-day period or longer based on a 30-year baseline daily climatology (here 1985–2014). We calculated a temperature climatology in each box, using temperature over the SML which was then volume-averaged (over the depth of the SML and per region). These climatologies were used for MHW identification. Individual events that were separated by one or 2 days were amalgamated into a continuous event, as per the definition. Seasonality of the MHWs was determined based on the month the first day of each MHW occurred.

2.3. Heat Budget

To investigate and compare the mechanisms modulating temperature variability in the mixed layer we calculated the terms of a daily heat budget following the methodology of Elzahaby et al. (2021) where the heat budget was defined based on Stevenson and Niiler (1983) as follows:

$$\frac{1}{h} \int_h^0 \frac{dT}{dt} dz = -\frac{1}{h} \int_h^0 \mathbf{u} \cdot \nabla_H T dz + \frac{1}{h} \int_h^0 \frac{Q_{net} - q(h)}{\rho c_p h} dz + Residual, \quad (1)$$

where h corresponds to the SML depths in each of the scenarios outlined above, $\frac{dT}{dt}$ is the temperature tendency and $\mathbf{u} \cdot \nabla_H T$ is the horizontal advection. Q_{net} is the net air-sea flux (such that positive fluxes are directed into the ocean), and ρ and c_p (1027 kg m^{-3} and $3850 \text{ J (kg C)}^{-1}$) are the water density and specific heat capacity, respectively. The heat loss by the shortwave radiation that penetrates below the depth h is given by $q(h)$ assuming an exponential decay of surface shortwave radiation with 25 m e-folding depth (Wang and McPhaden, 1999; Schlundt et al., 2014). The residual term accounts for vertical advection and horizontal and vertical diffusion. This term also includes computational error.

Daily climatologies (mean values for each day of the year over the study period) and anomalies (deviations from the daily climatology) were calculated over each model grid cell in each box for all terms in the heat budget, which were then volume-averaged (over the depth of the SML and per region) and integrated in time (over the duration of each MHW event) to produce a total anomaly per term for each event.

The dominant driver of the MHW was defined based on the dominant mechanism contributing to the change of temperature during the evolution of each event. More precisely, following the methods outlined in Elzahaby et al. (2021), a MHW was classified as Adv'-MHW (Q' -MHW) if the total advection (air-sea heatflux) anomaly over the duration of each event was dominant (similar to methods used in Chen et al., 2015; Bowen et al., 2017). If the difference between the contribution of Adv' and Q' was 10% or

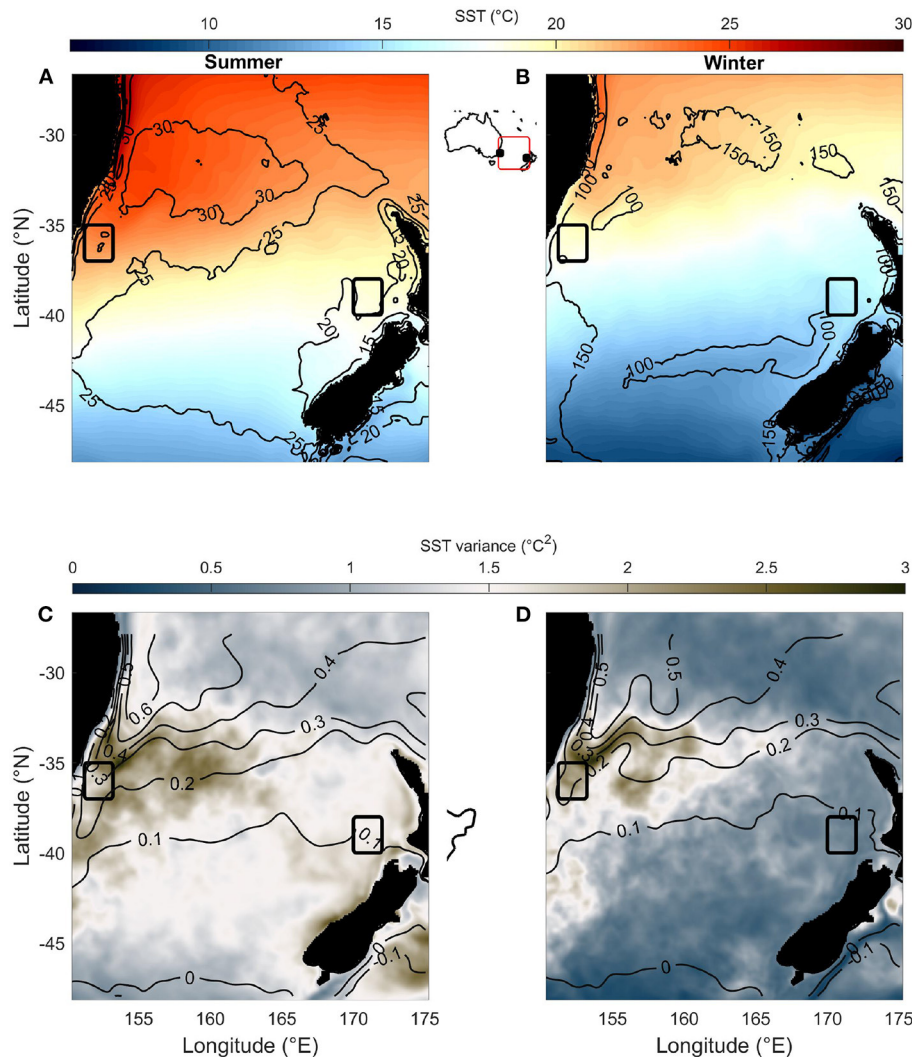


FIGURE 1 | Mean sea surface temperature (SST) from the Bluelink OFAM3 model during the summer months (**A,C**) and winter months (**B,D**) SST [colorbar, (**A,B**)] with MLD contours (m). Panels (**C,D**) show the SST variance with SLA contours. Values are based on the mean of the 30-year study period (1985–2014). The two boxes analyzed in the study are marked with black rectangles, Eddy box is on the left and NZ box on the right. An orientation map shows the study boxes in context.

less, the event was classified as “mixed” and was omitted in the summary analysis (Section 3.3).

2.4. Surface Mixed Layer Depth Estimates

We calculated the heat budget using three different depth estimates for the SML: (1) daily variable MLD based on de Boyer Montégut et al. (2004) (MLD_V), readily available from model output, (2) a fixed SML depth of 30 m (MLD_{30}) and (3) a fixed SML depth of 150 m (MLD_{150}). We chose the two fixed SML depths based on the region’s seasonal MLD signature. MLD_{30} corresponded to the mean summer MLD (20–40 m) which was then used to compare to the results of MLD_{150} , which encompassed the winter maximum MLD in the region (**Figure 1**).

To justify our choices of SML depth, the vertical structure of the SML is shown in **Figure 2** and the seasonal cycle of

the SML is shown in **Figure 3** for the two boxes. Overall, MLD_{30} intersected the high range of temperature and salinity variability in the mixed layer, whilst MLD_{150} encapsulated the total SML, on average (**Figure 2**). The daily varying SML depth shows the large annual MLD range (**Figure 3**) in both boxes.

Using the three different SML depths for the heat budget (MLD_{30} , MLD_V , and MLD_{150}), the primary driver of each MHW event was classified to analyse the sensitivity of the MHW driver detection to variability in the SML depth. Given the term magnitude dependence on the value of h (Equation 1), especially the air-sea heatflux term, we expected the balance between the magnitude of the terms in each of the scenarios to vary and, therefore, impact the identification of dominant drivers during MHWs. These ideas are explored below.

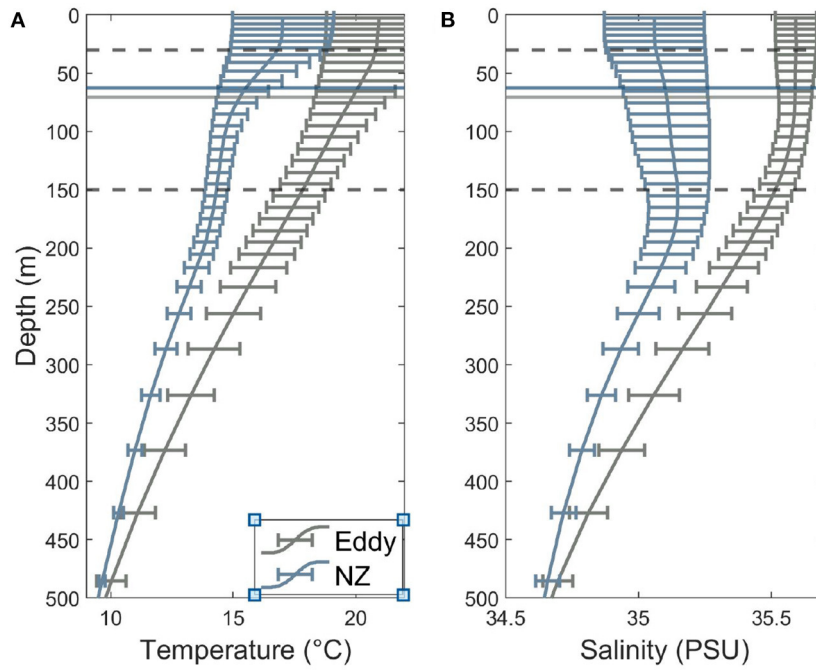


FIGURE 2 | Mean temperature **(A)** and salinity **(B)** for the Eddy box (grey) and NZ box (blue). MLD₃₀ and MLD₁₅₀ are marked by dashed black lines and the mean SML depth (MLD_v) per region is marked by solid horizontal lines.

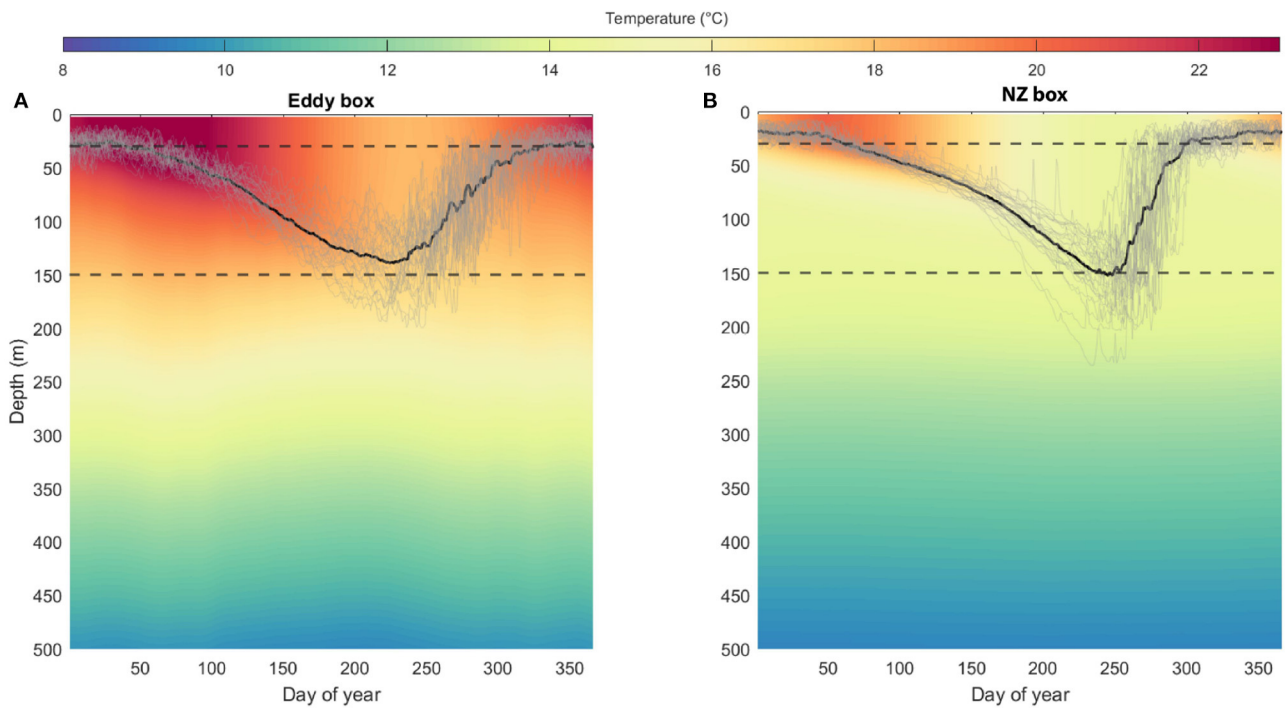


FIGURE 3 | Climatological temperature variability (colorbar) from the surface down to 500 m depth in the Eddy **(A)** and NZ boxes **(B)**. Mean SML depth is marked with solid black lines on each of the plots while the grey lines show annual SML depths for the 30 year period from 1985 to 2014.

3. RESULTS

3.1. Case Studies

Focusing on the dynamical evolution surrounding MHW events over the course of a single year, **Figure 4** shows the temporal evolution of the heat budget terms in the Eddy box during 2007. Three MHWs were identified in April (19 days), May (5 days), and December (5 days). The advection of anomalously cold water in February/March was followed by a deep, warm advection anomaly in March-May (**Figure 4C**). The first MHW occurred as a result of deep, strong, anomalously warm advection (Adv' , **Figure 4C**). Air-sea heatflux anomaly (Q' , **Figure 4A**) was relatively negligible (approximately neutral temperature contribution compared to 1.6°C from the advection term over the duration of the event) and, unsurprisingly, the event was classified as an Adv' -MHW in all three SML depth scenarios.

During the second event, pronounced Q' was detected in both MLD_{30} and MLD_V reaching a maximum of $\sim 0.12^{\circ}\text{C day}^{-1}$ and $\sim 0.05^{\circ}\text{C day}^{-1}$, respectively (and $<0.02^{\circ}\text{C day}^{-1}$ in MLD_{150}). During this event, the varying SML depth was approximately 70 m. In the SML, Adv' averaged $0.01^{\circ}\text{C day}^{-1}$, however, a warmer advection signal was detected below the SML ($>0.05^{\circ}\text{C day}^{-1}$). In this case, MLD_{30} overestimated the relative contribution of Q' whilst MLD_{150} captured the warm advection below the SML that was not contributing to the change of temperature in the mixed layer. Thus, the event was classified as Q' mixed (near equal contribution of anomalous advection and air-sea heatflux) and Adv' -MHW using the MLD_{30} , MLD_V , and MLD_{150} , respectively.

The final MHW in 2007 occurred during summer when the varying SML depth was approximately 20 m and the warm temperature anomaly was mostly restricted to the SML (**Figure 4E**). Throughout the whole water column, Adv' was negligible whilst Q' exhibited a significant signal in both MLD_{30} and MLD_V and as such the three scenarios classified this event as a Q' -MHW.

During the first event, negative density anomaly was associated with a deepening of the thermocline which can be observed during the May MHW (deepest isopycnal deflecting downwards, **Figure 4F**). The surface was fresh and warm (**Figures 4B,E**) but the anomalous warming extended well throughout the water column (as deep as 650 m). This warming was negligible on the 28.3kgm^{-3} potential density line (equivalent to 500 m isobar) suggesting water-mass conservation and possibly isopycnal heaving (**Supplementary Figure 1**). The surface snapshot shows that a warm-core eddy occupied the region which supports the possibility of heaving (**Figure 5A**) and confirms advection as the driver. During the second event, the warming depth extent on isobars also exceeded that on isopycnals but to a lesser extent compared to the first event (**Supplementary Figure 1**) with the region appearing to be enveloped by a meandering of warm currents (**Figure 5B**). The third event, driven by Q' , exhibited a strong spice signal (density compensated temperature and salinity gradients, Bindoff and McDougall (1994), **Figure 4D**) and density anomaly (**Figure 4F**) in the SML. The event appeared to be a part of an almost Tasman Sea region-wide MHW (**Figure 5C**).

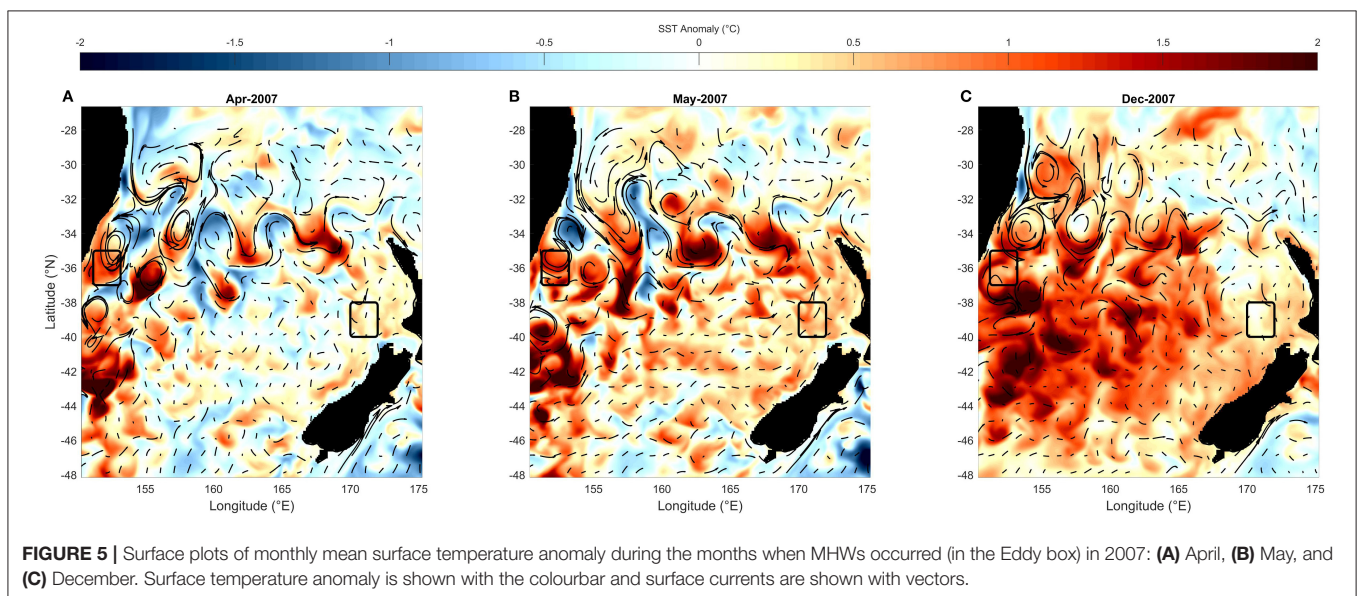
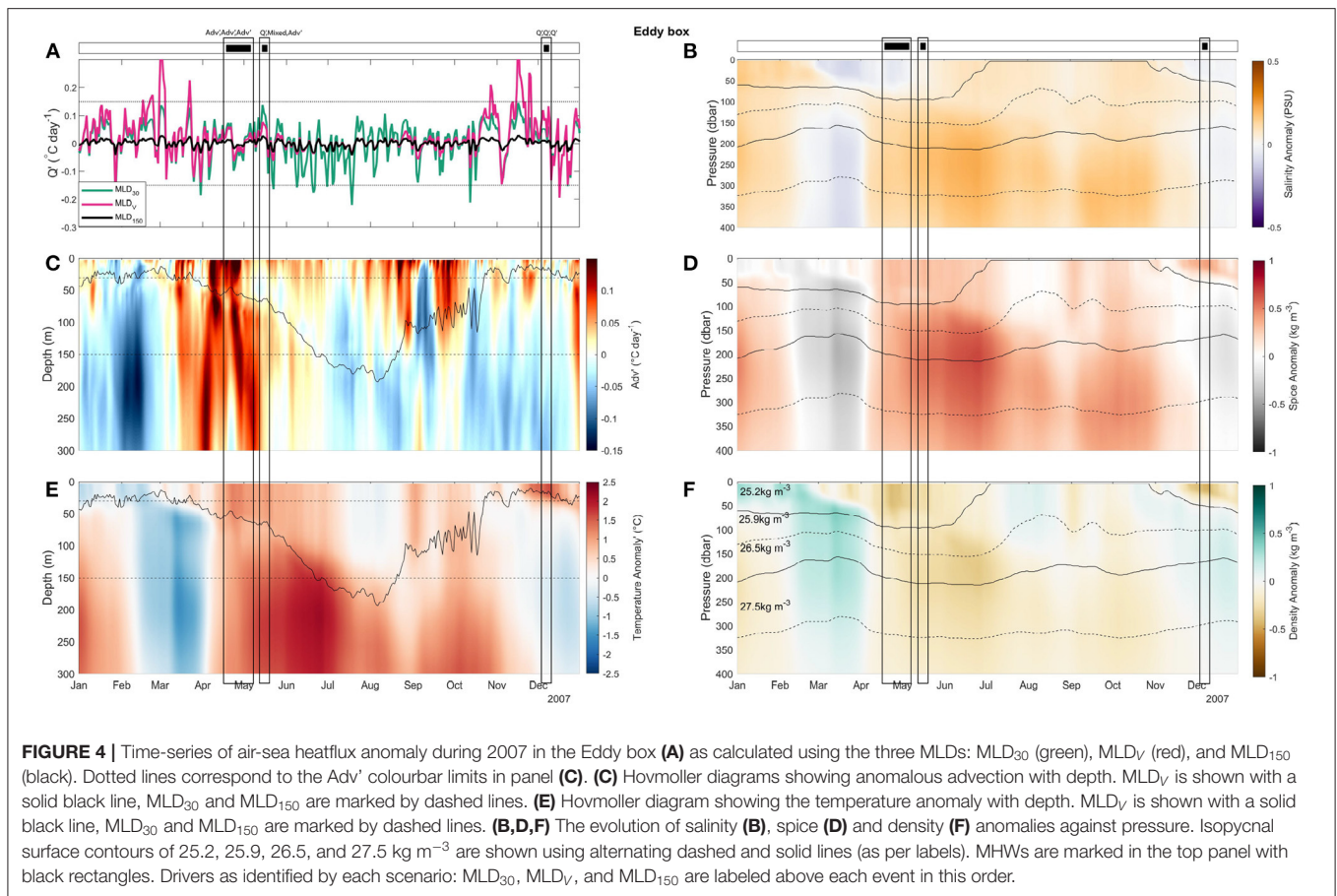
Our second case study focusses on 1998 off the west coast of New Zealand. Three MHWs occurred in 1998 during the months of February (11-days), March (5-days), and November (8-days) (**Figure 6**). The first event appeared in highly stratified water with warming affecting the SML only, whilst the denser and cooler January water-mass detrained below the mixed layer (**Figure 6E**). During the first two events, significant Q' was detected and reached maximums of $\sim 0.28^{\circ}\text{C day}^{-1}$ and $\sim 0.15^{\circ}\text{C day}^{-1}$ in February and March, respectively (**Figure 6A**). The varying SML depth was ~ 10 m and, thus, MHW_V represented the largest magnitude of Q' during both these events. Nonetheless, given the negligible contribution of Adv' in the region (**Figure 6C**), both events were classified as Q' -MHWs across all three SML depth scenarios. In contrast, the November MHW was classified differently in each of the scenarios. The varying SML depth during this event was, also, shallow (~ 20 m). Relatively mild Adv' and significant Q' was detected in the surface layers which was classified as a Q' -MHW using the MLD_V scenario (20 m average SML depth). MLD_{30} underestimated the Q' contribution and, thus, classified this event as a mixed-driven MHW. Whilst, MLD_{150} further underestimated Q' to the point that it was negligible compared to the mild positive Adv' in the SML and throughout the water column and, accordingly, the event was classified as an Adv' -MHW.

Spice anomalies were particularly weak during these MHWs compared to the Eddy region, indicating potential water mass transformation rather than compensation between salinity and temperature anomalies with the exception of a slight signal elevation during the first and last events. The surface maps of monthly mean temperature anomaly (**Figure 7**) show that in all three MHWs in this region, the events appear during region-wide extreme warming.

3.2. Role of MLD on Heat Budget Term Estimates

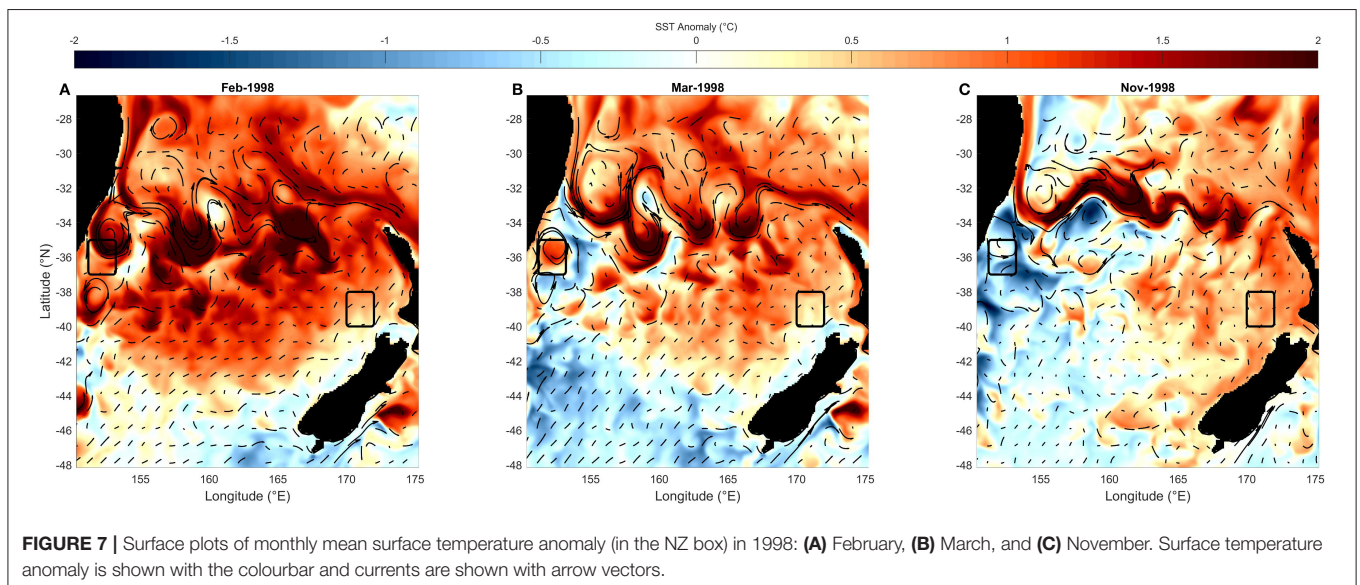
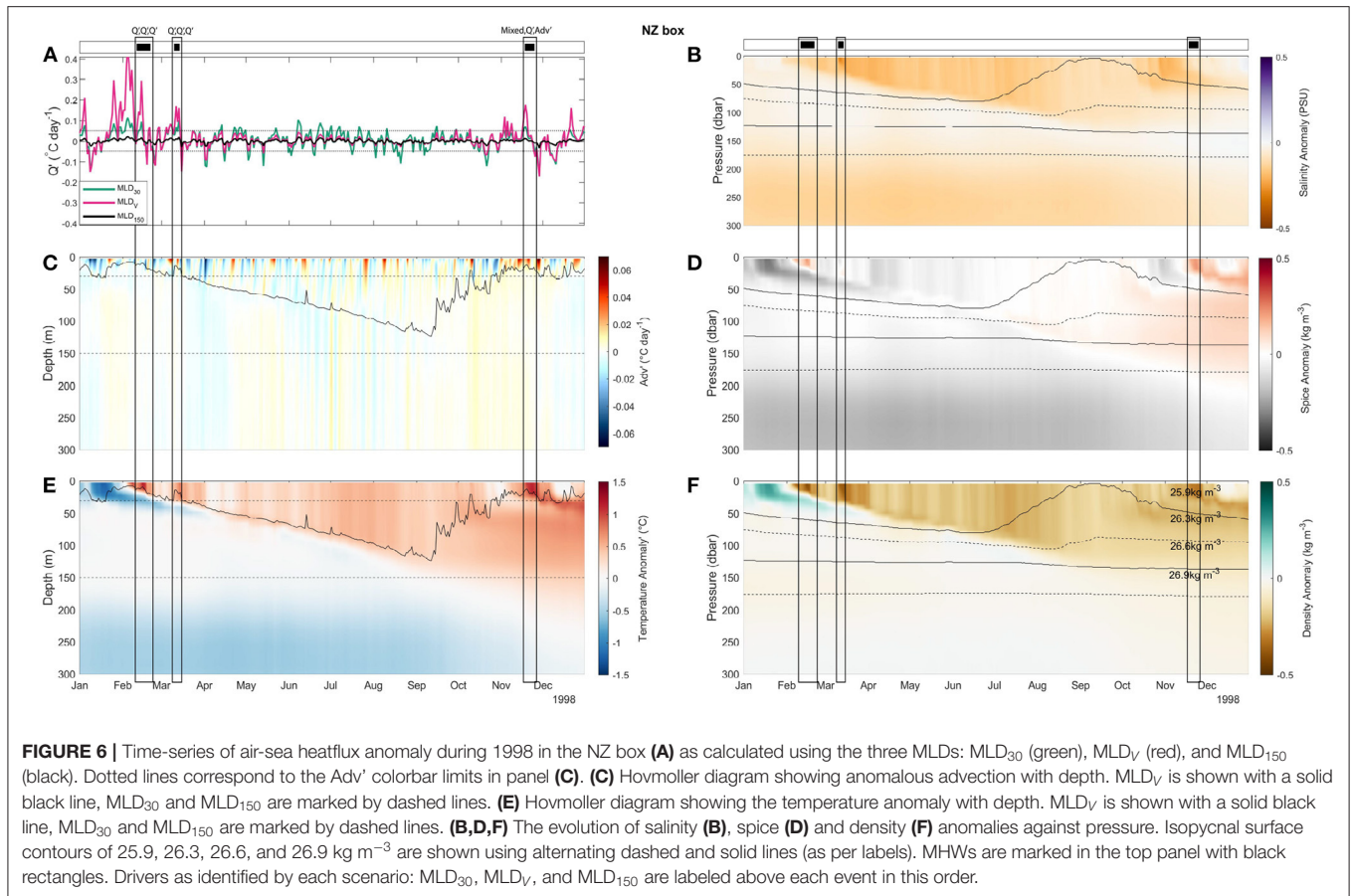
Next, we explore the statistical distribution of the magnitude of each heat budget term across the 30 years (1985–2014) in the three SML depth scenarios (**Figure 8**). In the Eddy region, on average, advection warmed the box while air-sea heatflux cooled the region as shown by the positive median value for the advection term (Adv) in **Figures 8A,C,E**. However, the relative magnitudes of the terms varied in the three SML depth scenarios. For the MLD_{30} scenario, the standard deviation of the residual was found to be of equivalent magnitude to that of the temperature tendency term whilst the air-sea heatflux term's standard deviation was approximately 1.5 times the magnitude of the temperature tendency's, on average (**Table 1**). This implied that some significant terms (e.g., the vertical terms) were not resolved in this scenario and that the impact of the air-sea heatflux term on the change of temperature was being overestimated. Consistent with the results found in the Eddy box, MLD_{30} in NZ also overestimated the air-sea heatflux term and produced a residual term equivalent in magnitude to the temperature tendency term.

For the MLD_V scenario in the Eddy box, air-sea heatflux, advection and temperature tendency terms all had similar



distributions whilst the residual was approximately half their magnitude. This suggests that the advection and air-sea heatflux terms were sufficiently descriptive of the temperature variability in the SML. In the NZ box, the MLD_V produced an equivalent magnitude of heat budget term distributions for

air-sea heatflux and temperature tendency while the residual term was much smaller (half the magnitude of the other terms at most), suggesting that in this region, the change of temperature with time can be sufficiently described by atmospheric forcing.



The MLD₁₅₀ scenario in the Eddy region produced similar relative term magnitudes as the MLD_v scenario for all terms except air-sea heatflux, which had an equivalent magnitude to the residual term. That is, the role of air-sea heatflux on the SML temperature was underestimated in this scenario. So,

although the small residual suggests that the terms were mostly resolved, the air-sea heat flux contribution to the temperature variability in the SML is unlikely to be properly represented. In the NZ region, the MLD₁₅₀ budget appeared to reasonably represent the budget terms. The air-sea heatflux term was

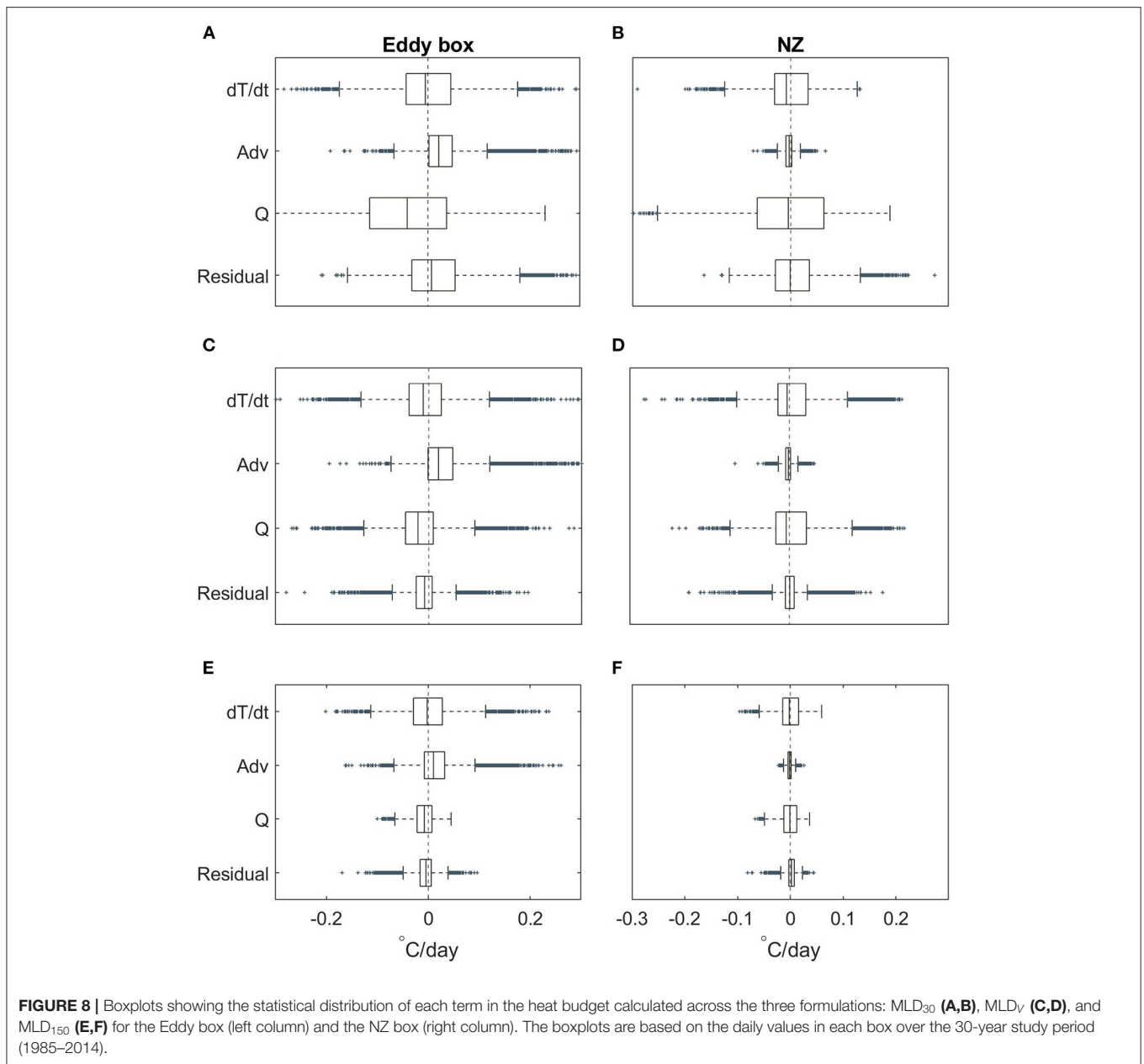


FIGURE 8 | Boxplots showing the statistical distribution of each term in the heat budget calculated across the three formulations: MLD₃₀ (A,B), MLD_v (C,D), and MLD₁₅₀ (E,F) for the Eddy box (left column) and the NZ box (right column). The boxplots are based on the daily values in each box over the 30-year study period (1985–2014).

TABLE 1 | Standard deviations (°Cday⁻¹) of the heat budget terms calculated in each of the three SML depth scenarios in the Eddy and NZ regions.

	Eddy			NZ		
	MLD ₃₀	MLD _v	MLD ₁₅₀	MLD ₃₀	MLD _v	MLD ₁₅₀
dT/dt	0.07	0.06	0.04	0.05	0.05	0.02
$u \cdot \nabla_H T$	0.05	0.05	0.04	0.01	0.01	0.005
Q	0.11	0.06	0.02	0.08	0.05	0.02
Residual	0.07	0.03	0.02	0.05	0.02	0.01

similar in magnitude to the temperature tendency term and the residual was half that magnitude on average, again, with negligible advection.

To demonstrate the sensitivity of the heat budget terms to the SML estimate, **Figure 9** (Eddy box) and **Figure 10** (NZ box) illustrate the temporal evolution of the terms in each of the scenarios (equivalent figures with term anomalies shown in **Supplementary Figures 2 and 3**). The time-series of each of the terms in the Eddy region show advection was not always constrained within the surface and, sometimes, extended deep in the water column. Advection was highly variable and barotropic.

In the New Zealand region, advection played a very small role in the temperature variability in the mixed layer. The time-series of each of the heat budget terms show that the influence of advection in this region was very small when compared to air-sea heatflux in all three scenarios. Across both regions, MLD₁₅₀ produced the smallest magnitude of the air-sea heatflux term

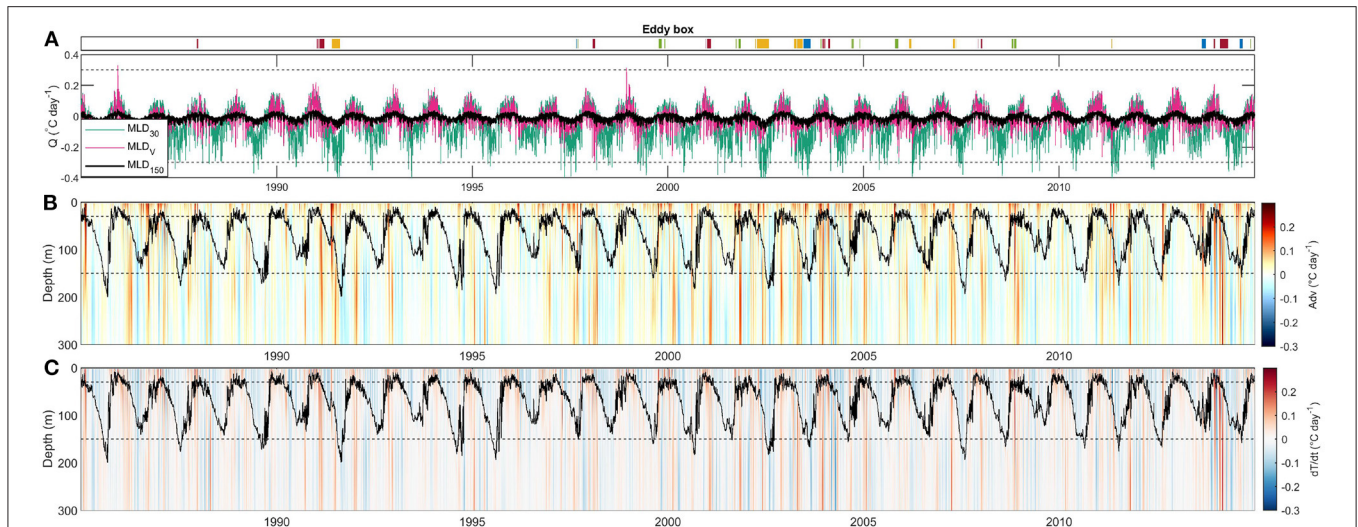


FIGURE 9 | Eddy box time-series (1985–2014) showing the air-sea heatflux term **(A)** as calculated using the three SML scenarios: MLD_{30} (green), MLD_V (red), and MLD_{150} (black). Hovmoller plots shows advection contribution **(B)** and temporal change of temperature **(C)** with depth. MLD_V is shown with a solid black line, MLD_{30} and MLD_{150} are marked by dashed lines. MHWs are marked with rectangles in the top bar with colors corresponding to the season in which an event began: summer (DJF) = red, autumn (MAM) = yellow, winter (JJA) = blue, spring (SON) = green.

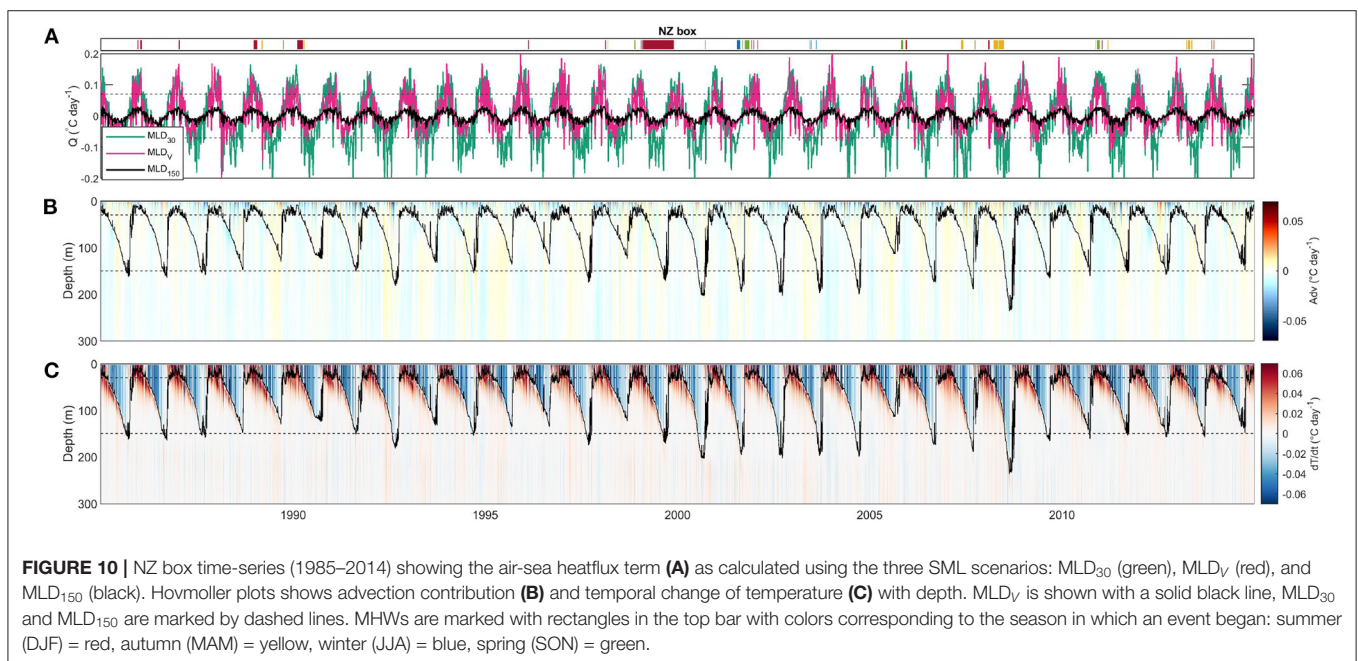


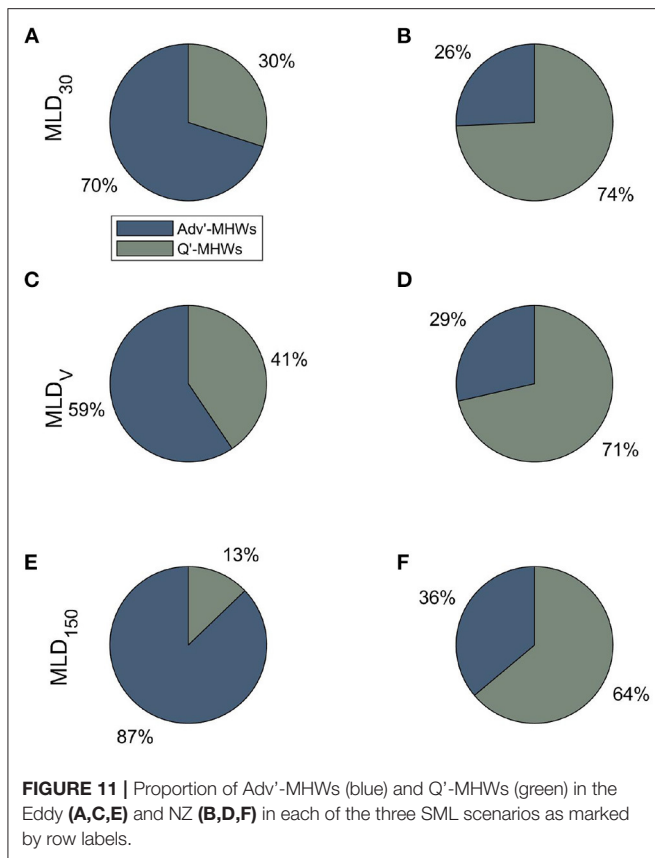
FIGURE 10 | NZ box time-series (1985–2014) showing the air-sea heatflux term **(A)** as calculated using the three SML scenarios: MLD_{30} (green), MLD_V (red), and MLD_{150} (black). Hovmoller plots shows advection contribution **(B)** and temporal change of temperature **(C)** with depth. MLD_V is shown with a solid black line, MLD_{30} and MLD_{150} are marked by dashed lines. MHWs are marked with rectangles in the top bar with colors corresponding to the season in which an event began: summer (DJF) = red, autumn (MAM) = yellow, winter (JJA) = blue, spring (SON) = green.

(Figures 9A, 10A). During the cool months, MLD_{30} produced the largest magnitude of the cooling air-sea heatflux term, whilst during the warm months some extreme warm contributions were only represented in the MLD_V scenario.

3.3. Role of MLD in Identifying Drivers of MHWs

The relative magnitude of the terms in the heat budget for the various SML scenarios were explored to understand the influence on the identification of the dominant drivers during MHWs. We detected 41 MHWs in the SML in each of the regions.

However the magnitude of the heat budget terms, and hence the classification of each of these MHW drivers changed across the three different SML scenarios (Figure 11). Overall, in the Eddy region MLD_V resulted in the largest number of Q' -MHWs when compared to the other two scenarios (41% compared to 30% and 13% using MLD_{30} and MLD_{150} , respectively), whilst MLD_{150} resulted in the largest number of Adv' -MHWs (87% compared to 70% and 59% classified by MLD_{30} and MLD_V , respectively) (Figures 11A,C,E). In the NZ box, MLD_{30} and MLD_V produced similar numbers of Q' -MHWs (74% and 71%, respectively) whilst MLD_{150} resulted in the largest number of



Adv'-MHWs (36% compared to 26 and 29% produced by MLD₃₀ and MLD_V, respectively).

As the depth of the SML changes throughout the year, we explored the classification of the MHW drivers by month and the temporal evolution of the heat budget terms (Figure 12). MLD₁₅₀ consistently classified the least number of Q'-MHWs and the most Adv'-MHWs throughout the year in both regions (marked with green lines in Figures 12E,F). In the Eddy region, MLD₁₅₀ classified ~2.8 Adv'-MHWs per month compared to ~1.8 Adv'-MHWs classified by MLD_V, on average. In the same region for Q'-MHWs, MLD₁₅₀ classified ~0.4 Q'-MHWs per month compared to 1.25 classified by MLD_V, on average. This difference is the least pronounced in May (austral autumn). In the NZ region, on average, MLD₁₅₀ classified ~1.1 Adv'-MHWs per month compared to MLD_V which classified 0.5 Adv'-MHWs per month. MLD₁₅₀ classified 1.9 events as Q'-MHWs on average per month compared to 2.7 classified using MLD_V. The gap between the three scenarios in their classification was the least pronounced during the months of July-September (winter-spring).

MLD₃₀ showed pronounced seasonality in its driver identification. In the Eddy region, over the autumn and summer periods when the MLD is shallow, the results were consistent with the relationship identified above, being that a deep estimate of SML resulted in a reduced (increased) number of Q'-MHWs (Adv'-MHWs). Given that this region is characterized with relatively deep MLD (average MLD during these months was

~45m), the number of Q'-MHWs was higher in the MLD₃₀ scenario compared to MLD_V (1.5 compared to 1.2) and the number of Adv'-MHWs was lower (2.3 compared to 2.5). During the cooler months (over the winter and spring seasons) the pattern is inverted. The MLD₃₀ produced a larger number of Adv'-MHWs than MLD_V (2.3 compared to 1.2, respectively) and a smaller number of Q'-MHWs (0.5 compared to 1.3, respectively) despite it being a shallower depth than the SML. That is, a shallow SML estimate resulted in an increased number of Adv'-MHWs and a reduced number of Q'-MHWs indicating that surface advection could be skewing the results toward classifying the events as Adv'-MHWs.

In the NZ region, the SML was mostly shallower than 30 m in the warmer months (~20 m in summer with a minimum of ~10 m and maximum of ~40 m). Thus, MLD_V produced the largest number of Q'-MHWs during the warmer months compared to the MLD₃₀ (2.9 compared to 2) and fewer Adv'-MHWs (0.5 compared to 1). During the cooler months (winter and spring) the difference was, overall, less pronounced compared to the Eddy region since advection is weaker in the NZ region (Figure 10). There was a slightly smaller number of Q'-MHWs in the MLD₃₀ compared to MLD_V (2.3 and 2.5, respectively) but little to no difference in the Adv'-MHWs except during the months of October and November.

4. DISCUSSION

The heat budget is an informative tool that can be used to diagnose the mechanisms modulating the temperature variability in the SML during the evolution of MHWs. However, when using a simplified depth-integrated heat budget over the SML for the purpose of MHW dominant driver detection, the main assumptions need to be carefully considered and, in particular, the depth estimate of the SML.

Here, we analyzed the contributions of ocean advection and atmospheric processes (through the heatflux at the air-sea interface) to temperature variability in two dynamically contrasting regions of the Tasman Sea (Eddy and NZ boxes). The advection and air-sea heatflux terms of the heat budget were calculated using three different SML depth estimates, allowing us to compare the use of a fixed SML depth (set to the typical summer and winter thresholds, MLD₃₀ and MLD₁₅₀) to that of a more realistic daily varying SML depth calculated from density and temperature thresholds (MLD_V, de Boyer Montégut et al., 2004).

In the advection-dominated region (Eddy box), the air-sea heat flux term in the heat budget was dampened (had an equivalent standard deviation magnitude to that of the residual term and half of the temperature tendency term) in MLD₁₅₀ while the advection and temperature tendency terms were of comparable magnitudes. The opposite was true in the MLD₃₀ scenario, where the air-sea heatflux term was amplified (1.5 times the magnitude of the standard deviation of the temperature tendency term) and the advection term dampened (smaller

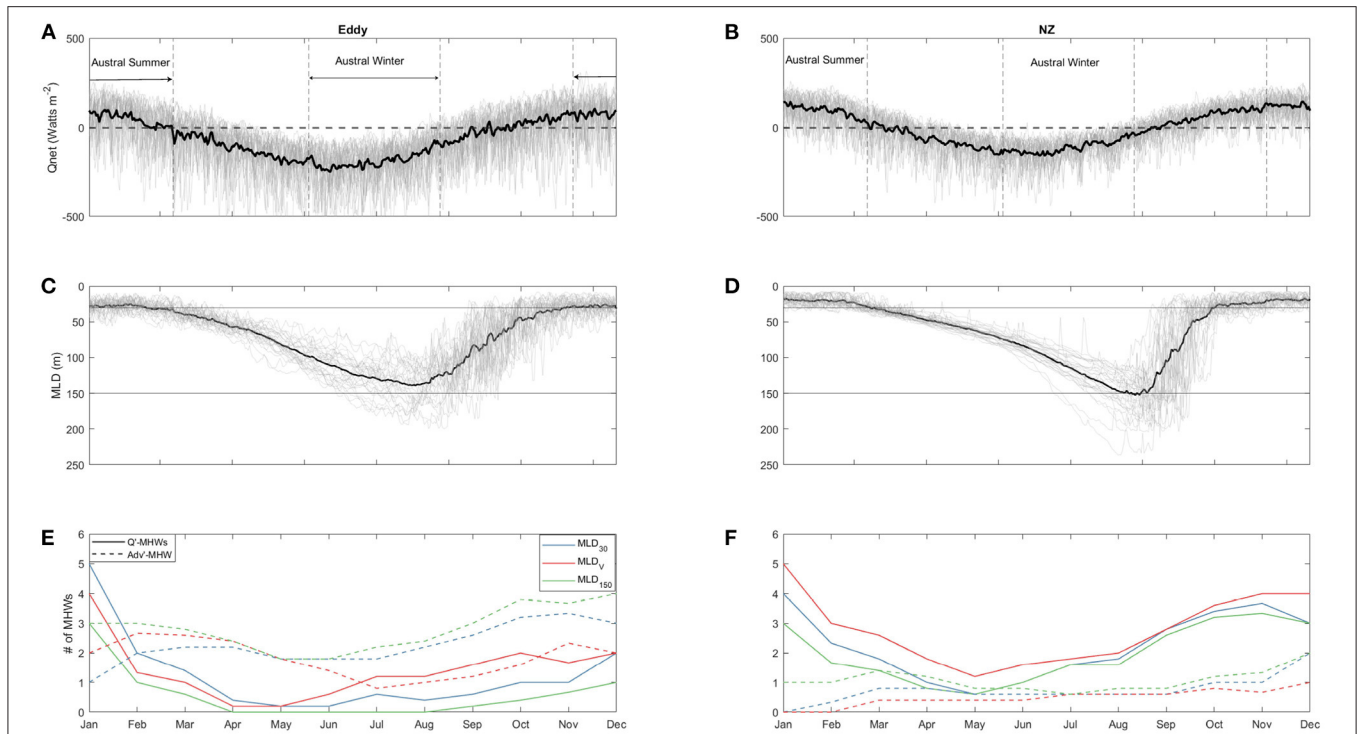


FIGURE 12 | Impact of seasonality on dominant driver classification of MHWs in the Eddy (**A,C,E**) and NZ (**B,D,F**) boxes. Mean annual air-sea heatflux is shown with thick black lines in panels (**A,B**) with gray lines illustrating the annual variability in the 1985–2014 (inclusive) period. Mean MLD is shown in panels (**C,D**) with annual variability also marked with gray lines. (**E,F**) show the number of MHWs identified as Q'-MHWs (solid lines) and Adv'-MHWs (dashed lines) in MLD₃₀ (blue), MLD_V (red), and MLD₁₅₀ (green) during each month.

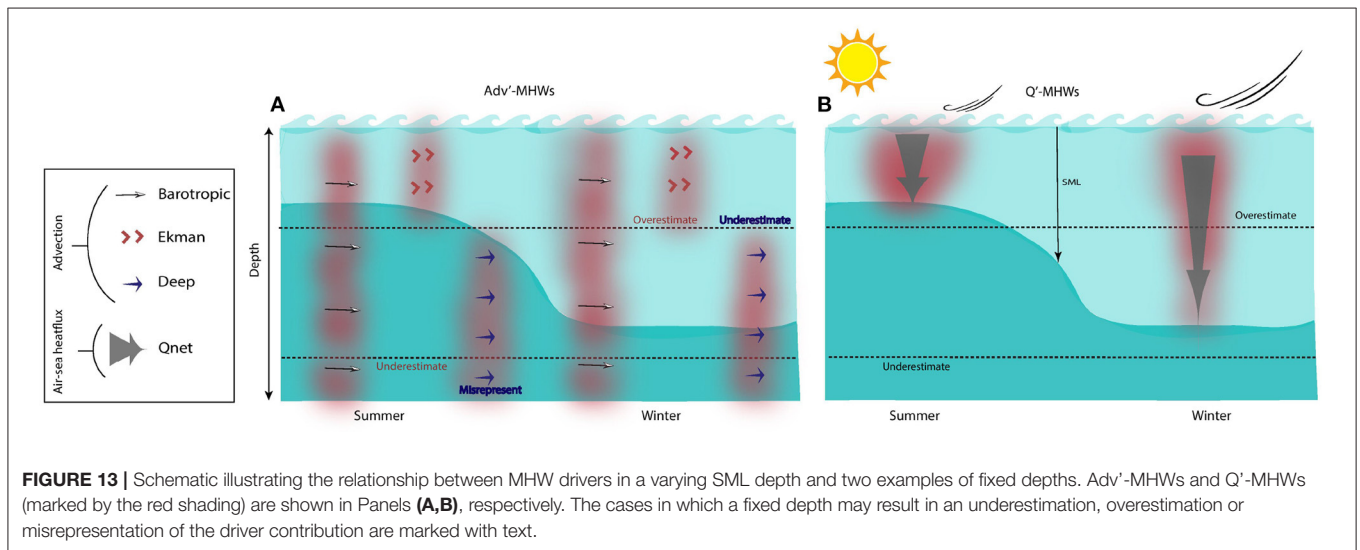


FIGURE 13 | Schematic illustrating the relationship between MHW drivers in a varying SML depth and two examples of fixed depths. Adv'-MHWs and Q'-MHWs (marked by the red shading) are shown in Panels (**A,B**), respectively. The cases in which a fixed depth may result in an underestimation, overestimation or misrepresentation of the driver contribution are marked with text.

magnitude than the residual term). The residual term in the MLD₃₀ scenario had an equivalent magnitude to the temperature tendency term which implied that not all processes modulating the change of temperature were resolved in this budget. In comparison, the benchmark scenario (MLD_V) represented the air-sea heatflux, advection and temporal change of temperature

terms at nearly equal magnitudes with the residual term at half that magnitude.

In the air-sea heatflux-governed region (NZ box), the advection term played a minor role in the budget and is relatively small regardless of the SML estimate. The air-sea heatflux term was amplified in the MLD₃₀ scenario (1.6 times

the standard deviation magnitude of the temperature tendency term) compared to being at equivalent magnitude in the MLD_V and MLD_{150} scenarios. The residual term in MLD_{30} is equivalent to the temperature tendency term, consistent with the Eddy box results, suggesting that the mechanisms modulating the temperature variability in the SML were not resolved. MLD_V and MLD_{150} represent similar relative term magnitudes with air-sea heatflux at equivalent magnitude to the temperature tendency term and residual at half that magnitude.

We, also, explored the impact of seasonality on driver detection across the three scenarios and found that, in general, a deep estimate of the SML resulted in a larger number of MHWs classified as Adv'-MHWs and a smaller number classified as Q'-MHWs across both regions with the biggest discrepancy being in the warmer months. An inverse pattern, however, was detected in the shallow budget (MLD_{30}) during the Austral winter months whereby a shallow estimate produced a larger number of Adv'-MHWs and a smaller number of Q'-MHWs with the difference being more pronounced in the Eddy region. MLD_{30} appeared to capture anomalous shallow surface warm advection which skewed the relative contribution of the air-sea heatflux and advection terms. Furthermore, despite MLD_{150} appearing to reasonably represent the budget terms in the NZ box, the extent to which the SML can shoal in this region during the Austral summer (up to 10 m, **Figure 3**) implies that this budget may fail to detect the drivers of summer MHWs.

Advection-driven MHWs in the SML are a result of anomalous warm ocean currents which could be due to strong geostrophic flow, surface Ekman currents, or eddies (Rebert et al., 1985). With the exception of Ekman currents, advection is not restricted to the surface and can be captured using various estimates of the SML regardless of season. However, our results show that air-sea heatflux-driven MHWs are sensitive to the estimate of SML since their detection is constrained to that depth. Penetrative shortwave radiation has a depth structure, albeit decaying at an exponential rate from the surface (Wang and McPhaden, 1999). The schematic in **Figure 13** illustrates the several cases in which Adv'- and Q'-MHWs can be misclassified or misconstrued. In summer, a deep approximation of the SML can result in surface advection contribution (Ekman flow) being underestimated. Conversely, in the winter months a shallow estimate of the SML depth may result in the amplification of the advection contribution to the SML warming. In the case where warm anomalous advection is detected below the mixed layer, a deep estimate of the SML may misrepresent it as a surface mechanism. A deep estimate of the SML depth dilutes the contribution of the air-sea heatflux anomaly and can cause mixed layer warming that is driven by air-sea heatflux in the summer months to be missed. On the other hand, in the winter months, a shallow estimate can result in amplifying the term's contribution to the SML warming.

Being able to accurately restrict the heat budget analysis to the temporally varying mixed layer enables the inter-comparison of dynamically contrasting regions. Since the SML depth is linked to a region's dynamical signature, we have shown that it is unlikely that a common fixed MLD can appropriately represent the mechanisms impacting the temperature variability

across the regions (see SML variability in **Figure 1**). As in our findings, despite MLD_{30} (MLD_{150}) having resulted in amplified (dampened) air-sea heatflux term compared to the temperature tendency term on average in both regions (**Figure 8**), the identification of an event's dominant driver was highly dependent on the region's dynamical signature. In the Eddy box, Adv'-MHWs outnumbered those in MLD_V in both cases of fixed depths (MLD_{30} and MLD_{150}). In the New Zealand region, the number of Q'-MHWs in the two fixed scenarios was underestimated compared to MLD_V . Due to the significant anomalous advection in the Eddy region, a deep estimate of SML is more likely to classify events as advection-driven at the expense of air-sea heatflux-driven events. For example, Elzahaby et al. (2021) found that the dominant driver of MHWs in the EAC upstream to be Q'-MHWs, which may have been more difficult to detect in a fixed layer depth since deep anomalous advection is also prevalent in this region (**Supplementary Figure 4**). We, therefore, propose that a variable SML depth reduces the results' dependence on seasonality and a region's local dynamical regimes.

In some heat budget applications, capturing the variability of the mixed layer is less consequential to the results. For example, studies that focus on the temporal evolution of each term rather than identifying a dominant term, like Oliver et al. (2017) who investigated the driving mechanisms of the 2015/16 MHW in the Tasman Sea. The authors focused on the change of each term's cumulative anomaly (heat budget integrated over 100 m depth) and, as such, a SML depth estimate is inconsequential to the results. Furthermore, studies that use an overly deep estimate of the SML (encompassing the entire mixed layer, for example, Bowen et al., 2017) and, also, define MHWs in that depth can avoid ambiguity when relating deep drivers to the SML extreme warming. However in some cases, when authors use a heat budget approach across large geographic regions with different oceanic conditions, and/or over multiple seasons (e.g., Marin et al., 2021) this could result in a mis-classification of the MHW drivers if a fixed SML is used. In cases where shallow estimates of the SML are being used, a heat budget that resolves all the terms (including vertical diffusion) can produce a more accurate depiction of the mechanisms than a simplified budget.

A fixed SML estimate can be especially ambiguous in cases when MHWs are driven by the re-emergence of detrained persistent temperature anomalies or the shoaling of the SML. In the first instance, the re-emergence of anomalously warm water occurs over a period of several seasons (Alexander et al., 1999), thus, a fixed MLD approach would need to explicitly resolve vertical terms, otherwise, the driver may be undetected. Furthermore, shoaling of the mixed layer can result in an amplified impact from the air-sea heatflux anomaly which can, then, result in a MHW. The shoaling of the MLD acts on larger time-scales than the immediate effect of stratification from the surface warming (**Supplementary Figure 5**). Given the driver detection dependence on larger time-scales of SML variability, a fixed depth may not capture the potential impact of Q' and, thus, driver (**Figure 13B**). In summary these results

from two dynamically contrasting regions show that when comparing heat budget results over large spatial and temporal scales, a variable SML is necessary in order to accurately identify the driver.

DATA AVAILABILITY STATEMENT

Publicly available datasets were analysed in this study. This data can be found here: https://geonetwork.nci.org.au/geonetwork/417srv/eng/catalog.search#/metadata/f9007_2850_9392_7175.

AUTHOR CONTRIBUTIONS

YE conducted the analysis and generated the figures. All authors developed the conceptual framework and contributed to interpreting the results, writing, and editing the manuscript.

REFERENCES

- Alexander, M. A., Deser, C., and Timlin, M. S. (1999). The reemergence of SST anomalies in the north Pacific Ocean. *J. Clim.* 12, 2419–2433. doi: 10.1175/1520-0442(1999)012<2419:TROSAI>2.0.CO;2
- Benthuyzen, J., Feng, M., and Zhong, L. (2014). Spatial patterns of warming off western Australia during the 2011 Ningaloo Ni no: quantifying impacts of remote and local forcing. *Continental Shelf Res.* 91, 232–246. doi: 10.1016/j.csr.2014.09.014
- Benthuyzen, J., Oliver, E., Feng, M., and Marshall, A. G. (2018). Extreme marine warming across tropical Australia during Austral summer 2015–2016. *J. Geophys. Res. Oceans* 123, 1301–1326. doi: 10.1002/2017JC013326
- Bindoff, N. L., and McDougall, T. J. (1994). Diagnosing climate change and ocean ventilation using hydrographic data. *J. Phys. Oceanogr.* 24, 1137–1152. doi: 10.1175/1520-0485(1994)024<1137:DCCAOV>2.0.CO;2
- Bond, N. A., Cronin, M. F., Freeland, H., and Mantua, N. (2015). Causes and impacts of the 2014 warm anomaly in the NE Pacific. *Geophys. Res. Lett.* 42, 3414–3420. doi: 10.1002/2015GL063306
- Bowen, M., Markham, J., Sutton, P., Zhang, X., Wu, Q., Shears, N. T., et al. (2017). Interannual variability of sea surface temperature in the southwest Pacific and the role of ocean dynamics. *J. Clim.* 30, 7481–7492. doi: 10.1175/JCLI-D-16-0852.1
- Brainerd, K. E., and Gregg, M. C. (1995). Surface mixed and mixing layer depths. *Deep Sea Res. I Oceanogr. Res. Pap.* 42, 1521–1543. doi: 10.1016/0967-0637(95)00068-H
- Chen, D., Busalacchi, A. J., and Rothstein, L. M. (1994). The roles of vertical mixing, solar radiation, and wind stress in a model simulation of the sea surface temperature seasonal cycle in the tropical Pacific Ocean. *J. Geophys. Res.* 99, 20345. doi: 10.1029/94JC01621
- Chen, K., Gawarkiewicz, G., Kwon, Y.-O., and Zhang, W. G. (2015). The role of atmospheric forcing versus ocean advection during the extreme warming of the northeast U.S. continental shelf in 2012. *J. Geophys. Res. Oceans* 120, 4324–4339. doi: 10.1002/2014JC010547
- Chen, K., Gawarkiewicz, G. G., Lentz, S. J., and Bane, J. M. (2014). Diagnosing the warming of the northeastern U.S. coastal ocean in 2012: a linkage between the atmospheric jet stream variability and ocean response. *J. Geophys. Res. Oceans* 119, 218–227. doi: 10.1002/2013JC009393
- Condie, S. A., and Dunn, J. R. (2006). Seasonal characteristics of the surface mixed layer in the Australasian region: implications for primary production regimes and biogeography. *Mar. Freshw. Res.* 57, 569. doi: 10.1071/MF06009
- de Boyer Montégut, C., Madec, G., Fischer, A. S., Lazar, A., and Ludicone, D. (2004). Mixed layer depth over the global ocean: an examination of profile data and a profile-based climatology. *J. Geophys. Res.* 109, C12. doi: 10.1029/2004JC002378

FUNDING

This research was undertaken with the assistance of resources and services from the National Computational Infrastructure (NCI), which is supported by the Australian Government. This work is a contribution to the Moana Project (www.moanaproject.org) funded by the New Zealand Ministry of Business Innovation and Employment, contract number Meto1801. This research was supported by an Australian Government Research Training Program (RTP) Scholarship.

SUPPLEMENTARY MATERIAL

The Supplementary Material for this article can be found online at: <https://www.frontiersin.org/articles/10.3389/fclim.2022.838017/full#supplementary-material>

- Deser, C., Alexander, M. A., and Timlin, M. S. (2003). Understanding the persistence of sea surface temperature anomalies in midlatitudes. 16, 57–72. doi: 10.1175/1520-0442(2003)016<0057:UTPOSS>2.0.CO;2
- Dong, S., Sprintall, J., Gille, S. T., and Talley, L. (2008). Southern ocean mixed-layer depth from argo float profiles. *J. Geophys. Res.* 113, C6. doi: 10.1029/2006JC004051
- Elzahaby, Y., and Schaeffer, A. (2019). Observational insight into the subsurface anomalies of marine heatwaves. *Front. Mar. Sci.* 6, 745. doi: 10.3389/fmars.2019.00745
- Elzahaby, Y., Schaeffer, A., Roughan, M., and Delaux, S. (2021). Oceanic circulation drives the deepest and longest marine heatwaves in the East Australian Current system. *Geophys. Res. Lett.* 48, e2021GL094785. doi: 10.1029/2021GL094785
- Fathrio, I., Manda, A., Iizuka, S., Kodama, Y.-M., and Ishida, S. (2018). Ocean heat budget analysis on sea surface temperature anomaly in western Indian Ocean during strong-weak Asian summer monsoon. *IOP Conf. Ser. Earth Environ. Sci.* 149, 012014. doi: 10.1088/1755-1315/149/1/012014
- Feng, M., McPhaden, M. J., Xie, S.-P., and Hafner, J. (2013). La Niña forces unprecedented leewind current warming in 2011. *Sci. Rep.* 3, 1277. doi: 10.1038/srep01277
- Gawarkiewicz, G., Chen, K., Forsyth, J., Bahr, F., Mercer, A. M., Ellertson, A., et al. (2019). Characteristics of an advective marine heatwave in the middle Atlantic bight in early 2017. *Front. Mar. Sci.* 6, 712. doi: 10.3389/fmars.2019.00712
- Heath, R. (1981). Oceanic fronts around southern New Zealand. *Deep Sea Res. A Oceanogr. Res. Pap.* 28, 547–560. doi: 10.1016/0198-0149(81)90116-3
- Hobday, A., Alexander, L., Perkins, S. E., Smale, D. A., Straub, S. C., Oliver, E. C., et al. (2016). A hierarchical approach to defining marine heatwaves. *Prog. Oceanogr.* 141, 227–238. doi: 10.1016/j.pocean.2015.12.014
- Hobday, A., Oliver, E., Gupta, A. S., Benthuyzen, J., Burrows, M., Donat, M., et al. (2018). Categorizing and naming marine heatwaves. *Oceanography* 31, 162–173. doi: 10.5670/oceanog.2018.205
- Jackson, J. M., Johnson, G. C., Dosser, H. V., and Ross, T. (2018). Warming from recent marine heatwave lingers in deep British Columbia Fjord. *Geophys. Res. Lett.* 45, 9757–9764. doi: 10.1029/2018GL078971
- Kara, A. B. (2003). Mixed layer depth variability over the global ocean. *J. Geophys. Res.* 108, 3079. doi: 10.1029/2000JC000736
- Kara, A. B., Rochford, P. A., and Hurlburt, H. E. (2000). An optimal definition for ocean mixed layer depth. *J. Geophys. Res. Oceans* 105, 16803–16821. doi: 10.1029/2000JC900072
- Levitus, S. (1982). Climatological atlas of the world ocean. *EOS* 64, 962–963.
- Li, Z., Holbrook, N. J., Zhang, X., Oliver, E. C. J., and Cougnon, E. A. (2020). Remote forcing of tasman sea marine heatwaves. *J. Clim.* 33, 5337–5354. doi: 10.1175/JCLI-D-19-0641.1

- Marin, M., Bindoff, N. L., Feng, M., and Phillips, H. E. (2021). Slower long-term coastal warming drives dampened trends in coastal marine heatwave exposure. *J. Geophys. Res. Oceans* 126, e2021JC017930. doi: 10.1029/2021JC017930
- Mills, K., Pershing, A., Brown, C., Chen, Y., Chiang, F.-S., Holland, D., et al. (2013). Fisheries management in a changing climate: lessons from the 2012 ocean heat wave in the northwest Atlantic. *Oceanography* 26, 191–195. doi: 10.5670/oceanog.2013.27
- Monterey, G., and Levitus, S. (1997). “Seasonal variability of mixed layer depth for the world ocean,” in *NOAA Atlas NESDIS* (Washington, DC: U. S. Gov.), p. 100.
- Ohlmann, J. C., Siegel, D. A., and Gautier, C. (1996). Ocean mixed layer radiant heating and solar penetration: a global analysis. *J. Clim.* 9, 2265–2280. doi: 10.1175/1520-0442(1996)009<2265:OMLRHA>2.0.CO;2
- Oke, P. R., Griffin, D. A., Schiller, A., Matear, R. J., Fiedler, R., Mansbridge, J., et al. (2013). Evaluation of a near-global eddy-resolving ocean model. *Geosci. Model Dev.* 6, 591–615. doi: 10.5194/gmd-6-591-2013
- Oliver, E. C. J., Benthuyzen, J. A., Bindoff, N. L., Hobday, A. J., Holbrook, N. J., Mundy, C. N., et al. (2017). The unprecedented 2015/16 Tasman sea marine heatwave. *Nat. Commun.* 8, 16101. doi: 10.1038/ncomms16101
- Polovina, J. J., Mitchum, G. T., and Evans, G. T. (1995). Decadal and basin-scale variation in mixed layer depth and the impact on biological production in the central and north Pacific, 1960–88. *Deep Sea Res. I Oceanogr. Res. Pap.* 42, 1701–1716. doi: 10.1016/0967-0637(95)00075-H
- Rahmstorf, S. (1992). Modelling ocean temperatures and mixed-layer depths in the Tasman sea off the south island, New Zealand. *N. Z. J. Mar. Freshw. Res.* 26, 37–51. doi: 10.1080/00288330.1992.9516498
- Rebert, J. P., Donguy, J. R., Eldin, G., and Wyrki, K. (1985). Relations between sea level, thermocline depth, heat content, and dynamic height in the tropical Pacific Ocean. *J. Geophys. Res.* 90, 11719. doi: 10.1029/JC090iC06p11719
- Ridgway, K., and Dunn, J. (2003). Mesoscale structure of the mean East Australian Current system and its relationship with topography. *Prog. Oceanogr.* 56, 189–222. doi: 10.1016/S0079-6611(03)00004-1
- Rykova, T., and Oke, P. R. (2015). Recent freshening of the East Australian Current and its eddies. *Geophys. Res. Lett.* 42, 9369–9378. doi: 10.1002/2015GL066050
- Salinger, M. J., Renwick, J., Behrens, E., Mullan, A. B., Diamond, H. J., Sirguy, P., et al. (2019). The unprecedented coupled ocean-atmosphere summer heatwave in the New Zealand region 2017/18: drivers, mechanisms and impacts. *Environ. Res. Lett.* 14, 044023. doi: 10.1088/1748-9326/ab012a
- Scannell, H. A., Johnson, G. C., Thompson, L., Lyman, J. M., and Riser, S. C. (2020). Subsurface evolution and persistence of marine heatwaves in the Northeast Pacific. *Geophys. Res. Lett.* 47, e2020GL090548. doi: 10.1029/2020GL090548
- Schaeffer, A., and Roughan, M. (2017). Subsurface intensification of marine heatwaves off southeastern Australia: the role of stratification and local winds. *Geophys. Res. Lett.* 44, 5025–5033. doi: 10.1002/2017GL073714
- Schlundt, M., Brandt, P., Dengler, M., Hummels, R., Fischer, T., Bumke, K., et al. (2014). Mixed layer heat and salinity budgets during the onset of the 2011 Atlantic cold tongue. *J. Geophys. Res. Oceans* 119, 7882–7910. doi: 10.1002/2014JC010021
- Sen Gupta, A., Thomsen, M., Benthuyzen, J. A., Hobday, A. J., Oliver, E., Alexander, L. V., et al. (2020). Drivers and impacts of the most extreme marine heatwave events. *Sci. Rep.* 10, 19359. doi: 10.1038/s41598-020-75445-3
- Smale, D. A., Wernberg, T., Oliver, E. C. J., Thomsen, M., Harvey, B. P., Straub, S. C., et al. (2019). Marine heatwaves threaten global biodiversity and the provision of ecosystem services. *Nat. Clim. Change* 9, 306–312. doi: 10.1038/s41558-019-0412-1
- Stammer, D., Balmaseda, M., Heimbach, P., Kohl, A., and Weaver, A. (2016). Ocean data assimilation in support of climate applications: status and perspectives. *Annu. Rev. Mar. Sci.* 8, 491–518. doi: 10.1146/annurev-marine-122414-034113
- Stevenson, J. W., and Niiler, P. P. (1983). Upper ocean heat budget during the Hawaii-to-Tahiti shuttle experiment. *J. Phys. Oceanogr.* 13, 1894–1907. doi: 10.1175/1520-0485(1983)013<1894:UOHBDT>2.0.CO;2
- Tilburg, C. E., Subrahmanyam, B., and O’Brien, J. J. (2002). Ocean color variability in the Tasman sea. *Geophys. Res. Lett.* 29, 125-1–125-4. doi: 10.1029/2001GL014071
- Tranter, D. J., Parker, R. R., and Cresswell, G. R. (1980). Are warm-core eddies unproductive? *Nature* 284, 540–542. doi: 10.1038/284540a0
- Wang, W., and McPhaden, M. J. (1999). The surface-layer heat balance in the equatorial Pacific ocean. Part I: mean seasonal cycle. *J. Phys. Oceanogr.* 29, 1812–1831. doi: 10.1175/1520-0485(1999)029<1812:TSLHBI>2.0.CO;2
- Wernberg, T., Smale, D., Tuya, F., Thomsen, M., Langlois, T., De Bettignies, T., et al. (2013). An extreme climatic event alters marine ecosystem structure in a global biodiversity hotspot. *Nat. Clim. Change* 3, 78–82. doi: 10.1038/nclimate1627

Conflict of Interest: SD was employed by MetOcean Solutions.

The remaining authors declare that the research was conducted in the absence of any commercial or financial relationships that could be construed as a potential conflict of interest.

Publisher’s Note: All claims expressed in this article are solely those of the authors and do not necessarily represent those of their affiliated organizations, or those of the publisher, the editors and the reviewers. Any product that may be evaluated in this article, or claim that may be made by its manufacturer, is not guaranteed or endorsed by the publisher.

Copyright © 2022 Elzahaby, Schaeffer, Roughan and Delaux. This is an open-access article distributed under the terms of the Creative Commons Attribution License (CC BY). The use, distribution or reproduction in other forums is permitted, provided the original author(s) and the copyright owner(s) are credited and that the original publication in this journal is cited, in accordance with accepted academic practice. No use, distribution or reproduction is permitted which does not comply with these terms.